Journal of Catalysis 272 (2010) 253–261

Contents lists available at ScienceDirect

Journal of Catalysis

journal homepage: www.elsevier.com/locate/jcat

Preparation of a nonleaching, recoverable and recyclable palladium-complex catalyst for Heck coupling reactions by immobilization on Au nanoparticles

Jun-Nan Young, Tsao-Ching Chang, Shih-Chung Tsai, Lin Yang, Shuchun Joyce Yu *

Department of Chemistry and Biochemistry, National Chung, Cheng University, Ming Hsiung, Chia Yi 621, TAIWAN, ROC

ARTICLE INFO

Article history:
Received 19 February 2010
Revised 7 April 2010
Accepted 9 April 2010
Available online 15 May 2010

Keywords:
Supported catalyst
Palladium
Heck reaction
Gold nanoparticles
Recyclable catalyst

ABSTRACT

The loading of a palladium complex immobilized on the surface of Au nanoparticles (NPs) was controlled through coordination to a supported spacer ligand (SL = $S(CH_2)_{11}NHP(O)(2\text{-}py)_2$) to yield catalyst particles of the composition $(RS)_xAu(SL)_y(SL\text{–}PdCl_2)_z$ (SR = $S(CH_2)_7CH_3$; x:y:z = (0.31–2.3):1:(0.45–3.3)) with diameters of 3.1–4.9 nm. A fraction of the supported spacer ligands (23–69%) was left uncapped to capture any soluble Pd species resulting from leaching. These surface-bound Pd(II)-complex catalysts were highly effective for Heck reactions of iodobenzene and alkylacrylates, yielding a maximum turnover frequency (TOF) of 4.87×10^4 h^1. Their catalytic activity was three- to tenfold higher than that of their unbound counterparts. These hybrid catalysts could be dissolved and precipitated. They could be quantitatively recovered and effectively recycled 15 times without significant loss of reactivity. The recovered Au NP-supported palladium could be also dissolved, precipitated and isolated. Various spectroscopic analyses were performed to determine a surface-structure composition of $(RS)_xAu(SL)_1(SL\text{–}Pd^0)_{0.53}$.

1. Introduction

Nanocatalysis is one of the most exciting and rapidly growing subfields of nanoscience. Metal nanoparticle (MNP) catalysts can mimic metal-surface activation and catalysis at the nanoscale and are thought to be a bridge between homogeneous and heterogeneous systems, offering distinct and tunable chemical activity, specificity and selectivity [1–7]. Gold nanoparticles are one of the most studied MNPs in the field of nanocatalysis. Alkanethiolate-protected Au NPs have been shown to possess solid surfaces similar to the (1 1 1) surface of bulk gold [8,9]. These Au NPs also behave like soluble molecules, exhibiting both dissolvability and precipitability [10,11]. Therefore, alkanethiolate-protected Au NPs are good candidates as supports for metal-complex catalysts, with the MNP catalyst combining the advantages of both supported and homogeneous catalysts. Several recent reports by our group and others have demonstrated the successful use of Au NP-supported metal-complex catalysts for various organic transformations [12–18].

The Heck coupling reaction [19] is one of the most powerful tools in synthetic chemistry for constructing aromatic carbon–carbon bonds between complex organic molecules with potential industrial or pharmaceutical applications. Various forms of palladium have been reported to be useful catalysts or precatalysts for Heck coupling reactions over the past two decades [20–23]. However, most coupling protocols still rely on homogeneous Pd-complex catalysts, in particular those with phosphorus donor ligands; unfortunately, soluble palladium in such a form is not recyclable and is difficult to separate from the products. Additionally, significant PC bond cleavage has been observed with both mono- and bidentate phosphine complexes, causing severe catalyst decomposition at elevated temperatures [24–27]. In contrast, heterogeneous palladium catalysts have been primarily developed for their thermal stability, easy separation and feasibility of catalyst recycling [28–30]. However, there have been several reports indicating that the active form of palladium in many solid systems is actually a soluble Pd species resulting from leaching at high temperature [21]. Therefore, it would be very difficult to arrive at general conclusions or mechanistic insights for such a system. We describe herein the preparation and application of a highly efficient, recoverable and recyclable Heck catalyst system composed of Au NP cores with controlled amounts of Pd(II) complex functionalized on their surfaces in a well-defined manner. These hybrid catalysts can be dissolved and precipitated, so their structures and reaction chemistry can be easily investigated by solution-phase nuclear magnetic resonance (NMR) spectroscopy with a resolution typically obtained for soluble systems.

It has been noted that leaching is almost unavoidable for most supported Pd catalysts. The leached Pd, in either soluble or solid form, could contribute much of the activity for Heck reactions [31–33]. In this study, a flexible spacer ligand, $HS(CH_2)_{11}NHP(O)(2\text{-}py)_2$ (HSL), supported on the surface of Au colloids, was

* Corresponding author. Fax: +886 5 2721040.
E-mail address: chejyy@ccu.edu.tw (S.J. Yu).

0021-9517/$ - see front matter © 2010 Elsevier Inc. All rights reserved.
doi:10.1016/j.jcat.2010.04.005

designed to be less than fully palladated. A portion of the spacer ligands (23–69%) remained uncapped to capture any soluble Pd species if leaching occurs from one of the palladated surface spacer ligands. In addition, these Au NP-supported palladium-complex catalysts could be quantitatively recovered from the Heck reaction mixture. Spectroscopic characterization of the recovered Pd-containing Au NPs suggested a surface composition of $(RS)_xAu(SL)_y(SL–Pd^0)_z$. Moreover, without the problem of Pd leaching, these recovered Au NPs–SL–Pd(0) hybrid catalysts can be effectively recycled 15 times without significant loss of activity.

2. Experimental

2.1. General methods

All chemicals were used as supplied without further purification. Methyl sulfoxide (DMSO), NEt_3 and NPr_3 were dried over CaH_2; $CHCl_3$ was dried over $CaCl_2$ and were freshly distilled under a stream of nitrogen prior to use. $Pd(CH_3CN)_2Cl_2$ was synthesized by a modification of a previously reported procedure [34]. Ultraviolet–visible (UV–vis), infrared (IR) and electron-impact (EI) mass-spectral data were obtained in-house at Chung Cheng. Chromatographic purifications were performed by flash chromatography using silica gel (Aldrich 63–200 mesh). Yields of spacer ligands and Pd catalysts refer to isolated products and are the average of three runs.

2.2. Materials

The spacer ligand $HS(CH_2)_{11}NHP(O)(2\text{-}py)_2$ (**2**) was synthesized according to our previously published procedures [12]. The compound $HS(CH_2)_{11}N_3$ (0.5 g, 2.1 mmol) was added to a solution of $P(2\text{-}py)_3$ (0.5 g, 1.9 mmol) in wet CH_3CN (30 mL). The mixture was stirred for 16 h at 82 °C. The mixture was dried under vacuum to give a light yellow solid. The solid was extracted with hot hexane (4 × 30 mL), and the extract was dried to obtain a white solid **4** (0.68 g, 75% yield).

Mixed thiolate-protected Au NPs, $(RS)_xAu(SL)_y$ (**3**), were synthesized according to a previously reported procedure [12]. Freshly prepared octanethiolate-protected Au NPs (**1**, 75 mg) [35] were dissolved in degassed $CHCl_3$ (25 mL). To this solution was added spacer ligand **2** (60 mg, 0.15 mmol), and the reaction mixture was stirred for 16 h at 70 °C. The solution was concentrated to a minimum amount (0.5 mL) then was washed with hexane (3 × 50 mL). A degassed acetone solvent (150 mL) was added, and the solution was allowed to sit at room temperature for 1 h to allow gold colloid precipitation. Further precipitation from acetone was performed continuously until no more free ligand **2** could be detected by ^1H NMR spectroscopy. Centrifugation gave the colloids as black solid product **3** (60 mg).

The molecular palladium(II)-complex catalyst, $HOLPdCl_2$ (**6**), was synthesized according to a previously published procedure [12]. Compound $HO(CH_2)_{11}NHP(O)(2\text{-}py)_2$ (0.5 g, 1.3 mmol) was added to a solution of $Pd(CH_3CN)_2Cl_2$ (0.34 g, 1.3 mmol) in CH_3CN (30 mL). The mixture was stirred for 6 h at ambient temperature. All volatiles were removed to give **6** as a yellow solid (0.70 g, 95% yield).

The silica-supported Pd(II)-complex catalyst $(O)_3Si–L–PdCl_2$ (**7**) was synthesized according to our previously published procedure [36]. $PdCl_2$ (94 mg, 0.525 mmol) was added to a solution of $NHP(O)(2\text{-}py)_2$-functionalized polysiloxane (200 mg, 0.966 mmol of py) in CH_3CN (15 mL). The mixture was stirred at reflux for 24 h. All volatile substances were removed, and the residue was extracted with $CHCl_3$ (2 × 10 mL). The extract was dried to give **7** as a yellow solid with a yield of 260 mg (91% based on py).

2.3. Catalyst preparation

Au NP-supported Pd(II)-complex catalyst, $(RS)_xAu(SL)_y(SL–PdCl_2)_z$ (**4**): To a freshly prepared solution of Au NPs **3**, $(RS)_{0.77}Au–(SL)_1$ (60 mg) in $CHCl_3$ (30 mL) was added $Pd(CH_3CN)_2Cl_2$ (8 mg). The reaction mixture was stirred for 8 h at ambient temperature. The supernatant obtained from the resulting mixture was dried under vacuum. The crude product was washed with acetone (50 mL × 3) to give **4** in the form of $(RS)_1Au(SL)_1(SL–PdCl_2)_{0.57}$ as a black powder (40 mg).

2.4. Catalyst characterization

2.4.1. Transmission electron microscopy (TEM)

The catalyst particle size and morphology were examined by brightfield and darkfield JEOL JEM-2010 microscopy operating at an accelerating voltage of 200 kV and equipped with a Gatan imaging filter (GIF). Supported Au NP Pd-complex catalysts were dispersed in $CHCl_3$ or DMSO before subsequent deposition onto a copper grid coated with carbon followed by ambient drying. Histograms of particle-size distributions were obtained by measuring at least 120 randomly selected particles from at least five different micrographs for each sample analyzed.

2.4.2. ^1H NMR spectra of **4** and **5**

The ^1H NMR spectra were recorded at 27 °C in $CDCl_3$ or d^6-DMSO on a Bruker DPK-400-MHz spectrometer; coupling constants are reported in Hz. Chemical shifts are given in ppm relative to TMS (tetramethyl silane).

^1H NMR analysis of the Au NPs, $(RS)_xAu(SL)_y(SL–PdCl_2)_z$ (**4**): $CDCl_3$: δ = 0.84 (br, C*H*$_3$), 1.15–1.53 (br, C*H*$_2$), 2.98 (m, C*H*$_2$NH), 3.22 (m, C*H*$_2$NH–(Pd^{II})), 4.51 (m, N*H*), 7.36 (m, py), 7.58 (m, py-(Pd^{II})), 7.78 (m, py), 8.07 (m, py), 8.32 (m, py-(Pd^{II})), 8.73 (m, py), 9.27 (m, py-(Pd^{II})) ppm. The formula of $(RS)_1Au(SL)_1(SL–PdCl_2)_{0.57}$ was calculated by integration of the ^1H NMR resonance signals. d^6-DMSO: δ = 2.76 (m, C*H*$_2$NH), 2.92 (m, C*H*$_2$NH–(Pd^{II})), 5.46 (m, N*H*), 7.05 (m, N*H*–(Pd^{II})), 7.49 (m, py), 7.77 (m, py-(Pd^{II})), 7.95 (m, py), 8.25 (m, py), 8.67 (m, py), 9.10 (m, py-(Pd^{II})) ppm. The NMR signals of the terminal CH_3 protons of RS (δ = 0.84 ppm), the pyridyl protons of SL (δ = 8.73 ppm) and the pyridyl protons of $SLPdCl_2$ (δ = 9.27 ppm) were integrated against a 0.038 M internal standard iodoanisole to give the ratio of RS:SL:$SLPdCl_2$ = 1:1:0.57. Calculations based on the average particle size obtained by TEM (3.9 nm ± 0.4) and NMR integration gave an average of 2382 ± 735 gold atoms for each Au core. Based on the average diameter of Au particles obtained from TEM, the calculated numbers of 435 ± 134 RS, 435 ± 134 SL and 248 ± 76 $SLPdCl_2$ per Au particle were obtained.

^1H NMR analysis of the recovered Au NPs 5, $(RS)_xAu(SL)_1(SL–Pd^0)_{0.53}$: $CDCl_3$: δ = 0.85 (br, C*H*$_3$), 4.46 (m, N*H*), 7.34 (m, py (SL)), 7.78 (m, py (SL)), 7.86 (m, py (Pd^0)), 8.20 (m, py (SL)), 8.30 (m, py (Pd^0)), 8.75 (m, py (SL)), 9.09 (m, py (Pd^0)) ppm. The NMR signals of the pyridyl protons of SL (δ = 8.75 ppm) and the pyridyl protons of $SLPd^0$ (δ = 9.09 ppm) were integrated against a 0.038 M internal standard iodoanisole to give the ratio of SL:$SLPd^0$ = 1:0.53. Calculations based on the average size obtained by TEM (14.1 nm ± 3.4) and NMR integration gave an average of 112,592 gold atoms for each Au core. The average numbers of surface thiolate molecules per Au core were about 7570 SL and 4012 $SLPd^0$.

2.4.3. X-ray photoelectron spectroscopy (XPS) of **4** and **5**

The XPS spectra were obtained with a Kratos AXIS ULTRA DLD spectrometer equipped with a monochromatized Al Kα X-ray source ($h\nu$ = 1486.69 eV) at 75 W and 5 mA. The survey spectra and high-resolution spectra were obtained at analyzer pass-energy

values of 160 and 20 eV, respectively. All spectra were charge compensated using the C_xH_y component peak of the carbon 1s spectra at a binding energy (BE) of 285.00 eV as the reference peak [37]. XPS spectroscopic analysis can be utilized to measure the electronic state of a certain element that exists within a material. The binding energies of the $3d_{3/2}$ and $3d_{5/2}$ levels of palladium were found to be 343 and 337 eV, respectively, for Pd^{II} in **4**, and 341 and 335 eV for Pd^0 in **5**. The binding energies of the $4f_{5/2}$ and $4f_{7/2}$ levels of gold were found to be 88 and 84 eV, respectively, for the Au NP core in both **4** and **5**.

2.4.4. Palladium loadings on $(RS)_1Au(SL)_1(SL–PdCl_2)_{0.57}$ (4) obtained from ^1H NMR, atomic absorption (AA) and inductively coupled plasma-mass (ICP-MS) spectroscopy

AA spectra were recorded on a Perkin Elmer Analyst 200 spectrometer, and ICP-MS spectra were recorded on a PE-SCIEX ELAN 6100 DRC spectrometer. Integration of the ^1H NMR signals of **4** (iodoanisole as internal standard) gave the Pd loading of $(RS)_1Au(SL)_1(SL–PdCl_2)_{0.57}$ as 2.899×10^1 mmol Pd^{II}/g. AA analysis on the same sample gave a Pd loading of 2.821×10^1 mmol Pd^{II}/g. ICP-MS gave a Pd loading of 2.827×10^1 mmol Pd^{II}/g.

2.5. General procedure for catalytic Heck reactions

The colloidal gold-surface-bound palladium catalyst $(RS)_xAu(SL)_y(SL–PdCl_2)_z$ (**4**) was dissolved in DMSO (20 mL) to make a stock solution (2.36×10^{-3} mmol Pd). To 0.85 mL of the stock solution (containing 1.0×10^{-4} mmol Pd) was added 0.15 mL of DMSO, iodobenzene (2.04 g, 10 mmol), *n*-butyl acrylate (1.28 g, 10 mmol) and NEt_3 (1.5 mL). The reaction mixture was stirred for 3 h at 115 °C. After the reaction, the resulting tarry mixture was extracted with hexane (3×40 mL). The combined hexane extracts were washed with H_2O (3×40 mL) to remove salt by-products. All volatiles were removed under vacuum. The Heck product was further purified on a short silica plug to remove the catalyst (63–200 mesh; eluted with ethyl acetate). The product was used directly for NMR analysis.

2.6. Catalyst-recycling experiments

A mixture of iodobenzene (0.04 mmol), *n*-butyl acrylate (0.049 mmol), NPr_3 (0.08 mmol) and $(RS)_1Au(SL)_1(SL–PdCl_2)_{0.57}$ (**4**, 11.05 mg) in d^8-toluene (0.1 mL) was reacted at 108 °C for 30 min. The resulting mixture was centrifuged. The precipitate thus obtained was washed with dried hexane (0.5 mL × 5) to give Au NPs–Pd^0 as a black solid to be used in the following catalytic cycle. Recycling of $Pd(CH_3CN)_2Cl_2$ was performed under similar procedures. The detailed reaction conditions were as follows: iodobenzene, 0.375 mmol; *n*-butyl acrylate, 0.45 mmol; NPr_3, 0.75 mmol; 8 mol% $Pd(CH_3CN)_2Cl_2$; toluene, 0.1 mL; 110 °C; 6 h.

3. Results and discussion

3.1. Partial palladation on the surface of Au NPs

The incomplete metallation of the surface spacer ligand (SL = $S(CH_2)_{11}NHP(O)(2\text{-py})_2$) on Au NPs, $(RS)_xAu(SL)_y$ (**3**) (SR = $S(CH_2)_7CH_3$; $x{:}y$ = 1.43–0.77:1; D = 3.9 ± 0.4–4.7 ± 1.4 nm), was achieved by direct reaction with a limiting amount of $(CH_3CN)_2PdCl_2$ (0.2–0.8 equivalent to SL) to give the desired Au colloids, $(RS)_xAu(SL)_y(SL–PdCl_2)_z$ (**4**), ($x{:}y{:}z$ = 0.31–2.3:1:0.45–3.3; D = 3.1 ± 0.9–4.9 ± 0.8 nm) (Scheme 1). Leaving a portion (23–69%) of the supported ligands uncapped made the target hybrid system very soluble in many organic solvents, ranging from the relatively less polar $CHCl_3$ to the very polar DMSO. This made it very easy to manage when using solution-phase spectroscopy for quantitative or structural analysis. In contrast, fully palladated Au NPs are only partially soluble in DMSO [12], thus methods for their characterization and their application as supported catalysts for organic transformations have been limited.

The ^1H NMR analyses of **4** were performed in both $CDCl_3$ and DMSO to give spectra with resolutions typically obtained with soluble systems. As shown in Fig. 1d, the ^1H NMR spectra of **4** clearly showed two sets of spacer pyridyls: one from the uncapped spacer ligand (Au–SL) and the other from the palladated spacer ligand (Au–SLPdCl_2). The IR spectra of **4** also showed that the ν_{asym}(SH)

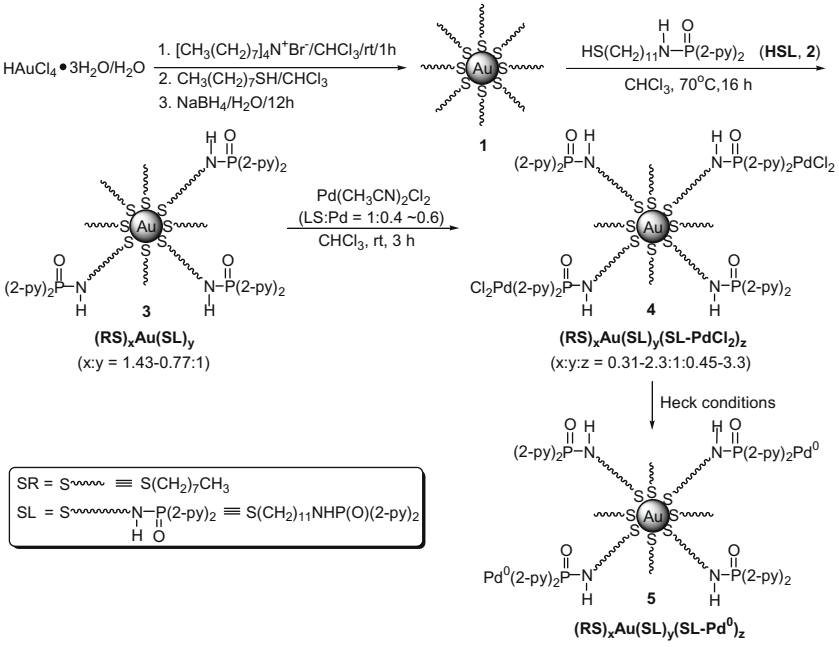

Scheme 1. Synthesis of Pd(II)-functionalized Au NPs, $(RS)_xAu(SL)_y(SL–PdCl_2)_z$ (**4**).

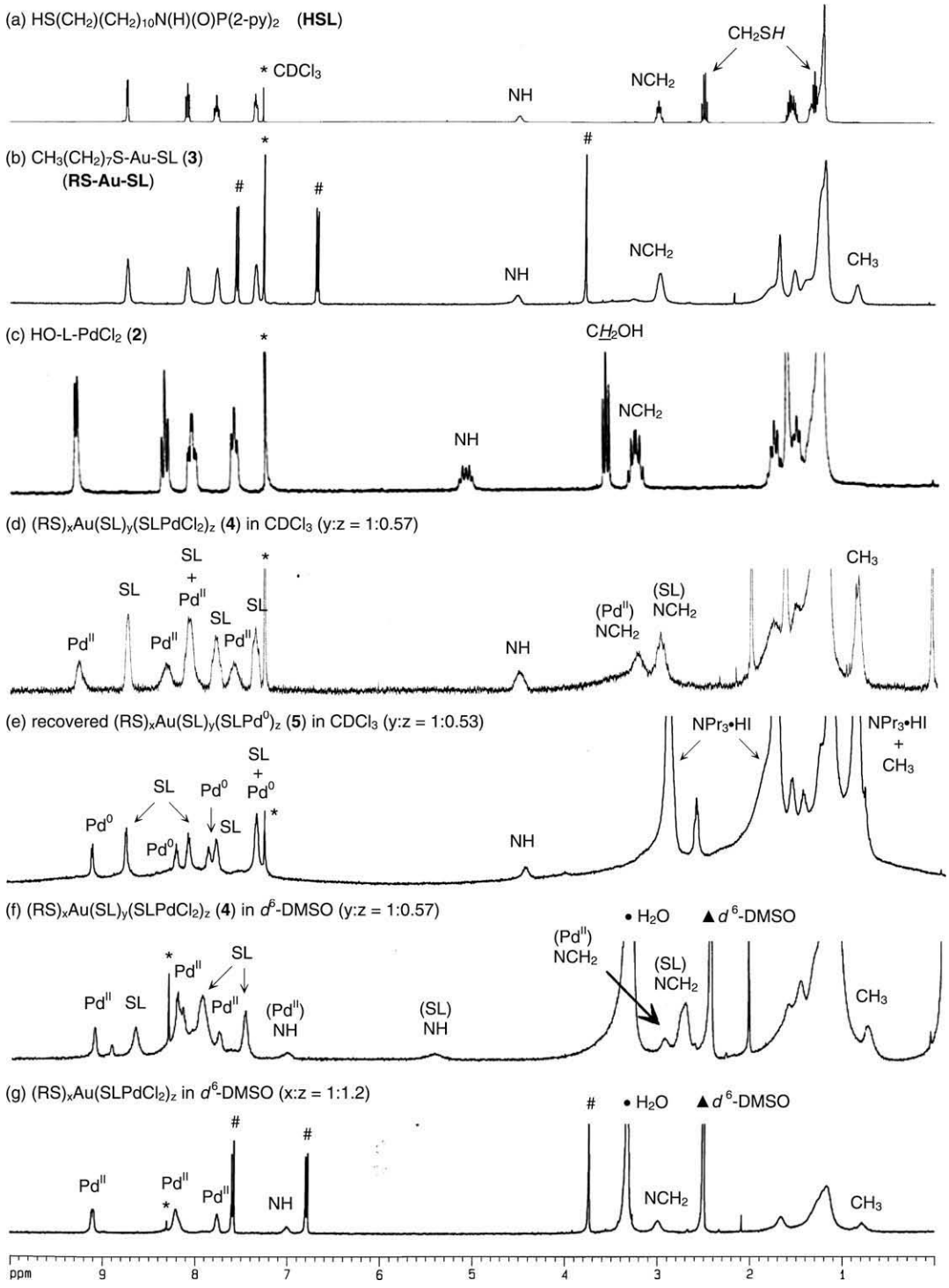

Fig. 1. The 400-MHz ^{1}H NMR (27 °C) spectra of (a) unbound spacer ligand HSL (**2**) in $CDCl_3$, (b) RS–Au–SL NPs (**3**) in $CDCl_3$, (c) molecular Pd complex **6** in $CDCl_3$, (d) $(RS)_{1.7}Au(SL)_1(SLPdCl_2)_{0.57}$ NPs (**4**) in $CDCl_3$, (e) $(RS)_xAu(SL)_1(SLPd^0)_{0.53}$ NPs (**5**) in $CDCl_3$ recovered from the **4**-catalyzed reaction of iodobenzene and *n*-butyl acrylate, (f) $(RS)_1Au(SL)_1(SLPdCl_2)_{0.57}$ NPs (**4**) in d^6-DMSO, and (g) fully $PdCl_2$-metallated Au NPs (RS–Au–$SLPdCl_2$) in d^6-DMSO (∗ is $CDCl_3$, # is the internal standard iodoanisole, ● is water, and ▲ is d^6-DMSO).

bands at 2569 cm^{-1} of the free *n*-octanethiol (HSR) and at 2576 cm^{-1} of the unbound free ligand (HSL, **2**) disappeared after their immobilization onto Au NPs (Fig. 2b). Moreover, a shift of the pyridyl ring stretching ν_{py} from 1574 to 1590 cm^{-1} indicated its covalent binding to palladium [12,36]. The UV–vis spectra of **4** gave the characteristic Au surface-plasmon resonance peak at ~520 nm (Fig. 3). The TEM images of **4** showed that partially Pd(II)-functionalized Au NPs were obtained, ranging in size from 3.1 ± 0.9 nm to 4.9 ± 0.8 nm, (Fig. 4 and Table 1). The XPS spectroscopic analysis of **4** (Fig. 5) showed the BE of the palladium $3d_{3/2}$ and $3d_{5/2}$ levels at 343 and 337 eV, respectively; these values are consistent with previously reported data for Pd(II) complexes [38]. The BE of the gold $4f_{5/2}$ and $4f_{7/2}$ levels of the Au core in **4** were found at 88 and 84 eV, respectively.

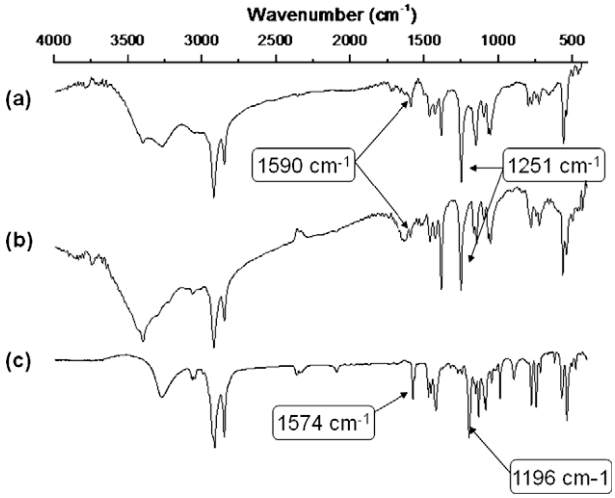

Fig. 2. IR spectra of (a) recovered catalyst Au NP **5**, (b) precatalyst Au NP **4**, and (c) ligand HSL ($HS(CH)_{11}NHP(O)(2\text{-}py)_2$).

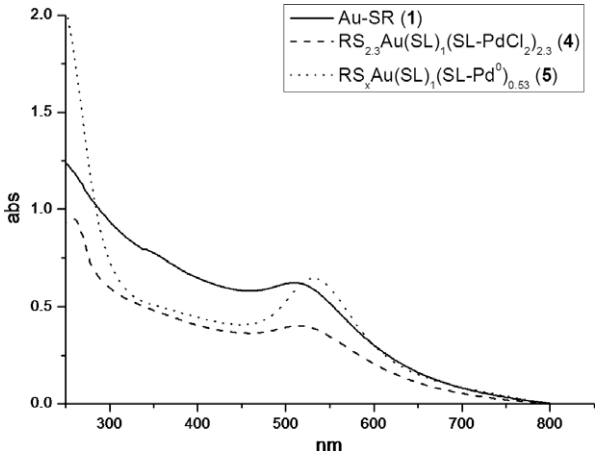

Fig. 3. UV spectra of Au NPs **1**, **4** and **5**.

The Pd(II) loadings on **4** as determined by either AA or ICP-MS spectroscopy were systematically smaller (<3%) than those obtained by ^{1}H NMR spectroscopy. One specific sample of **4** was analyzed by ^{1}H NMR to give a Pd loading of 2.899×10^1 mmol Pd^{II} per gram of Au NPs, while AA analysis on the same sample gave a Pd loading of 2.821×10^1 mmol Pd^{II}/g; ICP-MS analysis gave a Pd loading of 2.827×10^1 mmol Pd^{II}/g. As it required only 10 min to acquire a ^{1}H NMR spectrum (Fig. 1), we chose solution-phase NMR spectroscopy as the routine method for quantitative measurements and for in situ monitoring of reaction chemistry.

3.2. Catalytic Heck reactivity of the partially palladated Au NPs $(RS)_xAu(SL)_y(SL\text{–}PdCl_2)_z$ (**4**)

We found that both partially and fully palladated Au NPs were extremely effective catalysts for Heck reactions with iodobenzene and alkyl acrylates. The catalyses were carried out in DMSO or in a mixture of $CHCl_3$ and *o*-xylene at 115 °C. As shown in Table 2, the reactions of 10 mmol of iodobenzene and H_2C = CHR (R = COOMe, COOEt, COO^nBu, or COO^tBu) with NEt_3 (1.5 mL) and catalyst **4** (1×10^{-4} mmol of Pd^{II}) proceeded most efficiently in DMSO, giving Heck products with 89.3–97.3% yields in two hours and with TOFs of 44,700–48,700 h^1. Even with a nonactivated substrate such as styrene, the TOF was still as high as 18,700 h^1. The use of a less polar solvent also became convenient when trialkylamine was used as the organic base. However, the same catalyses gave lower TOFs in a mixture of $CHCl_3$ and *o*-xylene under similar reaction conditions (Table 2, entries 6 and 7). This was possibly because a better homogeneity could be achieved for the Pd-complex catalyst in a more polar media. In addition, a TOF of 234 h^{-1} could still be obtained even for the more difficult reaction of bromobenzene and *n*-butylacrylate. The best known TOF of 10^6 h^{-1} reported for the Heck reaction of iodobenzene and methylacrylate was catalyzed by the Pd-complex containing a six-membered CNN-pincer palladacyle [39]. However, it is interesting to note that this palladacycle was difficult to be recycled and was far less effective for the Heck reactions between bromobenzene and acrylic esters.

It has been reported that transition-metal complexes attached to monolayered-alkanethiolates on Au colloids exhibit catalytic properties similar to those of the corresponding homogeneous catalysts [14–18]. In the current study, $HO(CH_2)_{11}N(H)(O)P(2\text{-}py)_2PdCl_2$ (**6**) [12] (Scheme 2) and $Pd(CH_3CN)_2Cl_2$ were used as controls to study the effect of the immobilization of molecular Pd(II) on the surface of Au NPs. As demonstrated in Table 2, both Pd(II) complexes had similar reactivities. However, it is interesting to note that a significant increase in TOFs was observed when Pd(II) was immobilized onto the surface of Au NPs. When the gold core was covered only with octanethiolates (RS–Au NPs (**1**)), it was found to be noncatalytically active for Heck reactions. Addition of **1** to the Heck system containing molecular catalyst **6** did not provoke any further reactivity. Conversely, it reduced the TOFs of **6** from 4100–14,400 h^{-1} to 1100–2800 h^{-1}. This drop in reactivity was probably due to competitive substrate binding between the supported Pd centers and the relatively large number of surface Au atoms [12,40]. However, with the Pd(II) complex immobilized on

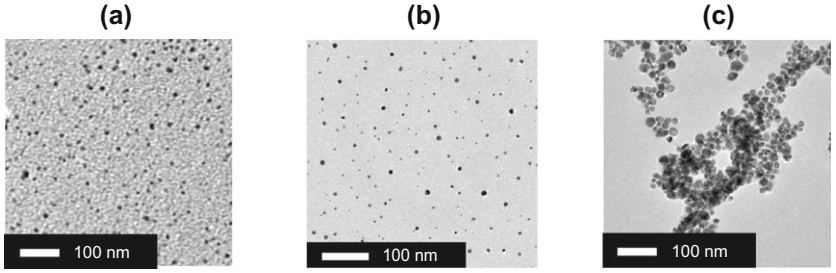

$(RS)_1Au(SL)_1(SL\text{-}PdCl_2)_{0.57}$ (**4**) D = 3.9 ± 0.4 nm

$(RS)_1Au(SL\text{-}PdCl_2)_{1.2}$ (**4**) D = 4.6 ± 0.86 nm

$(RS)_xAu(SL)_1(SL\text{-}Pd^0)_{0.53}$ (**5**) D = 14.1 ± 3.4 nm

Fig. 4. TEM images of Au NPs; (a) the partially palladated **4**, $(RS)_1Au(SL)_1(SL\text{–}PdCl_2)_{0.57}$; (b) the fully palladated **4**, $(RS)_1Au(SL\text{–}PdCl_2)_{1.2}$; (c) the recovered $(RS)_xAu(SL)_1(SL\text{–}Pd^0)_{0.53}$ (**5**).

Table 1
Analytical data of spacer ligand- and Pd-complex-functionalized Au NPs **3**, **4** and **5**.

Au NPs (m^2/core)	Particle size (nm)	Pd/SL/SR[a] mole ratio	Pd/Au_{total}[b] (wt.%)	$Au_{surface}$ atom%[c]	Pd/SL/SR[d] (molecule/core)	Surface area[e]
$(RS)_1Au(SL)_{1.1}$ (**3**)	4.1 ± 0.8	0/1/1.1	–	28.4	0/542/484	5.28×10^{-17}
$(RS)_1Au(SL)_1(SL–PdCl_2)_{0.57}$ (**4**)	3.9 ± 0.4	0.57/1/1	5.61 (5.46)	29.9	248/435/435	4.77×10^{-17}
$(RS)_1Au(SL–PdCl_2)_{1.2}$ (**4**)	4.6 ± 0.86	1.2/0/1	5.73 (5.51)	25.4	415/351/0	6.64×10^{-17}
$(RS)_xAu(SL)_1(SL–Pd^0)_{0.53}$ (**5**)	14.1 ± 3.4	0.53/1 (Pd^0/SL)	(1.93)	8.3	4012/7570 (Pd^0/SL)	6.24×10^{-16}

[a] Pd = Pd(II) complex on Au surface; SR = octanethiolate on Au surface.
[b] Weight percent of Pd(II)-to-total Au as determined by NMR; numbers in parentheses were obtained by atomic absorption analysis.
[c] Defined as the number of surface Au atoms (ns)/total number of Au atoms per particle (n) × 100%, where $ns = S/\pi \times (r^o)^2$.
[d] The average number of Pd(II) and octanethiol molecules per Au particle.
[e] Average surface area (S) of Au particles calculated by $S = 4\pi \times (r^o)^2 \times n^{2/3}$, where r^o = atomic radius of Au; n = average number of Au atoms per particle; $r = r^o \times n^{1/3}$, where r = average radius of Au particles.

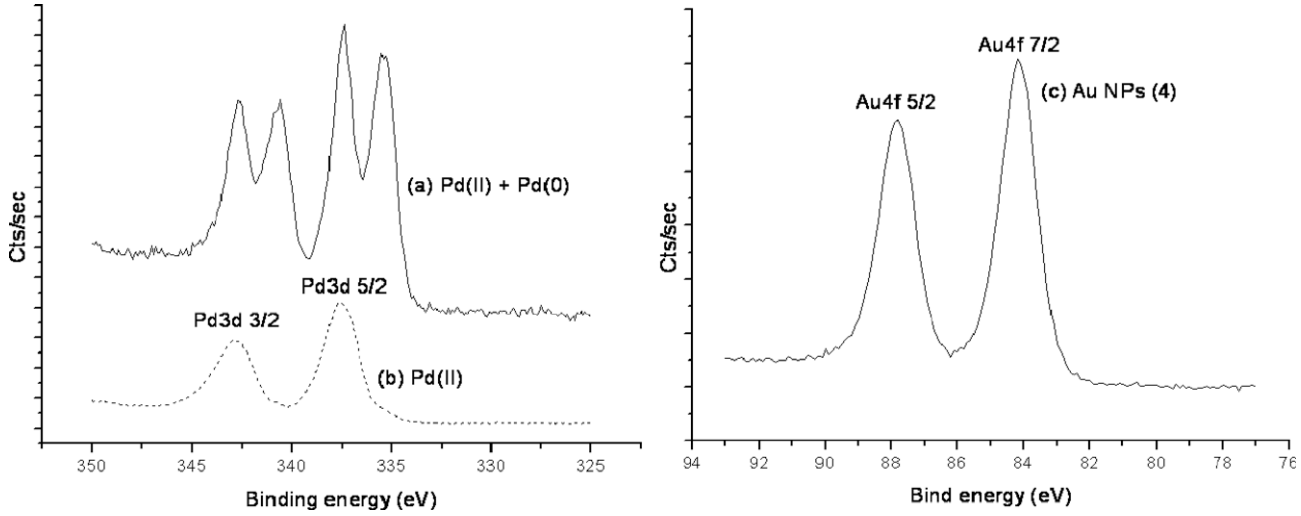

Fig. 5. Palladium 3d photoelectron spectra of (a) a 1:1 mixture of Au NPs $(RS)_1Au(SL)_1(SLPdCl_2)_{0.57}$ (**4**) and $(RS)_xAu(SL)_1(SLPd^0)_{0.53}$ (**5**); (b) Au NPs $(RS)_1Au(SL)_1(SLPdCl_2)_{0.57}$ (**4**); and (c) the gold 4f photoelectron spectra of the central Au core of **4** and **5**.

Table 2
Catalytic Heck-type coupling reactions mediated by Pd(II) in various forms.[a]

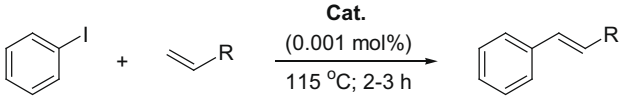

Entry	Catalyst system (**Cat.**)	TOF (h^{-1})/(yield (%))[f]				
		R=				
		COOMe	COOEt	COO^nBu	COO^tBu	Ph
1	$(RS)_1Au(SL)_0(SL–PdCl_2)_{1.2}$ (**4**)[b]	4.73×10^4 (94.7)	4.87×10^4 (97.3)	4.60×10^4 (92.0)	4.47×10^4 (89.3)	1.87×10^4 (37.3)
2	$(RS)_{2.3}Au(SL)_1(SL–PdCl_2)_{3.3}$ (**4**)[b]	3.79×10^4 (75.8)	3.94×10^4 (78.7)	3.67×10^4 (73.4)	3.65×10^4 (72.9)	1.50×10^4 (30.1)
3	$(RS)_1Au(SL)_1(SL–PdCl_2)_{0.57}$ (**4**)[c]	1.12×10^4 (33.7/3 h)	1.20×10^4 (35.9/3 h)	1.05×10^4 (31.4/3 h)	1.03×10^4 (30.8/3 h)	0.44×10^4 (13.2/3 h)
4	RS-Au NPs (**1**)[d]	0	0	0	0	0
5	$HO(CH_2)_1{}^1HNOP(2\text{-}py)_2PdCl_2$ (**6**)[b]	1.08×10^4 (21.5)	1.44×10^4 (28.7)	1.13×10^4 (22.5)	1.24×10^4 (24.8)	0.41×10^4 (8.2)
6	$Pd(CH_3CN)_2Cl_2$[b]	1.11×10^4 (22.2)	1.50×10^4 (30.0)	1.45×10^4 (29.0)	1.32×10^4 (26.3)	0.43×10^4 (8.5)
7	$Pd(CH_3CN)_2Cl_2$[c]	ND[g]	ND	0.10×10^4 (3.2/3 h)	ND	ND
8	**1** + **6**[d]	0.22×10^4 (6.5/3 h)	0.28×10^4 (8.3/3 h)	0.24×10^4 (7.1/3 h)	0.22×10^4 (6.5/3 h)	0.11×10^4 (3.4/3 h)
9	$(O)_3Si\text{-}L\text{-}PdCl_2$ (**7**)[e]	0.90×10^4 (27.0/3 h)	1.0×10^4 (30.0/3 h)	0.71×10^4 (21.3/3 h)	0.97×10^4 (29.0/3 h)	0.44×10^4 (13.1/3 h)

[a] Iodobenzene = 10 mmol; CH_2 = CHCOOR = 10 mmol; NEt_3 = 1.5 mL; 115 °C.
[b] $Pd^{II} = 1 \times 10^{-4}$ mmol; DMSO = 1 mL; 2-h reaction time.
[c] $Pd^{II} = 1 \times 10^{-4}$ mmol; $CHCl_3$/*o*-xylene = 1 mL (*v*:*v* = 1:1); 3-h reaction time.
[d] $Pd^{II} = 1 \times 10^{-4}$ mmol; DMSO = 1 mL; 0.2 mg of **1**; 3-h reaction time.
[e] $Pd^{II} = 3 \times 10^{-4}$ mmol; DMSO = 0.5 mL; 3-h reaction time.
[f] Isolated products were purified by flash chromatography, and TOF was determined by ^1H NMR spectroscopy.
[g] ND = not determined.

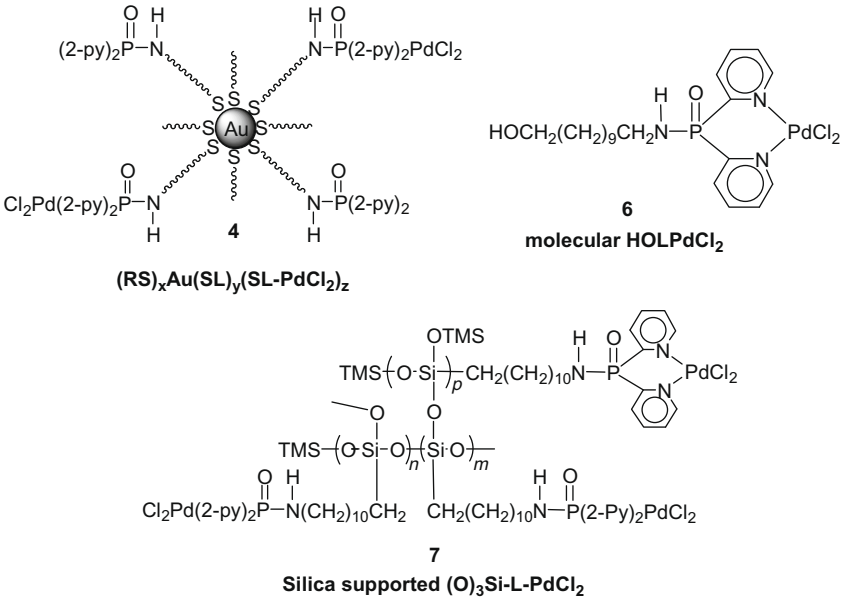

Scheme 2. Molecular and surface-supported palladium precatalysts.

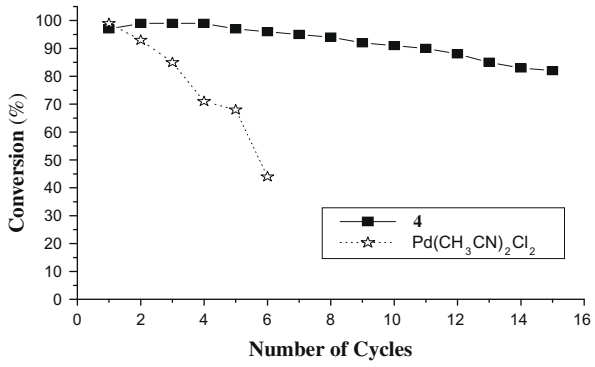

Fig. 6. Comparative recycling and reuse of precatalysts $(RS)_1Au(SL)_1(SLPdCl_2)_{0.57}$ (**4**) and $Pd(CH_3CN)_2Cl_2$ in the reaction of iodobenzene and *n*-butyl acrylate in d^8-toluene.

the surface of Au NPs, substrate binding to the surface Au atoms may possibly increase the local concentration of reactants around the supported Pd center and facilitate the catalysis. To verify the reactivity promotion of Au on Pd, we also studied the catalyses on a different surface. The SiO_2-bound Pd(II) complex, $\equiv(O)_3SiL\text{-}PdCl_2$ (**7**) (Scheme 2), was prepared according to our previously reported procedures [36]. In contrast to the case on the Au surface, the same Pd(II) complex supported on SiO_2 did not cause reactivity enhancement and only provided TOFs similar to those of its unbound free forms (Table 2).

It has been documented that composites of Pd/Au in various forms can greatly enhance the catalytic activity, selectivity and stability of Pd [12,41–43]. For example, adding gold to palladium in a bimetallic Pd–Au alloy system can significantly increase Pd catalytic activity in the acetoxylation of ethylene through an ensemble effect, in which the orientation of the Pd on Au surface favors formation of the product [44]. In addition, similar effects have also been demonstrated for gold colloids and gold-coated glass-slide-bound Ru(III) catalysts for the ring-opening metathesis polymerization of norbornene [45]. It was clearly seen in our case that the tethered Pd(II) complex and the surface Au atoms cooperated through immobilization in such a way as to give overall activities higher than either metal alone. However, as with most other reported occurrences, the promotional role of Au in our system has not yet been elucidated.

It is noteworthy that the TOFs observed with a fully palladated Au NP catalyst having no free Pd-binding ligand (Table 2, row 1) are about 25% greater than those from the partially palladated Au NP catalyst with free Pd-binding sites. The higher value does not seem attributable to leached Pd species, which are apparently less active than the bound ones. The exact cause for the higher TOFs observed for the fully palladated Au NP catalyst when compared with the partially palladated Au NP catalyst is not yet clear. However, it was noted in the catalyses that the fully palladated Au NP catalysts formed flocculates in DMSO, while the partially palladated Au NP catalyst formed a regular suspension in DMSO. The formation of flocculates may somehow have a positive influence on the catalytic performance of palladium. The study of the correlation between catalytic activity and flocculates formation is currently in progress.

3.3. Recovery of palladium and catalyst recycling

It is generally known that most current applications of homogeneous Pd catalysts cope with difficulties in quantitative separation, catalyst recovery and catalyst deactivation into inactive colloidal species at higher temperatures [46,47], while most heterogeneous Pd catalysts suffer from low TOFs and poor reusability due to either particle aggregation or leaching [48–54]. In the current study, filtration and split tests [23] were performed at the end of the **4**-catalyzed reaction of iodobenzene and butyl acrylate. The filtrate obtained after centrifugation and filtration of the reaction mixture was tested and found to have no residual Heck reactivity and no sign of palladium or gold content on AA spectroscopic analysis. Both results suggested that Pd leaching into either the active or inactive form did not occur. On the contrary, when fully palladated Au NPs $(RS)_1Au(SL)_0(SL\text{–}PdCl_2)_{1.2}$ were used in the recycling experiment, the filtrate obtained from the Heck reaction mixture still afforded a ~4% further conversion. This result suggested that a small amount of soluble Pd species was leached from the surface of the fully palladated Au NPs.

Table 3
Comparative recycling and reuse of precatalysts $(RS)_1Au(SL)_1(SL–PdCl_2)_{0.57}$ (**4**) and $Pd(CH_3CN)_2Cl_2$ in the Heck coupling reaction of iodobenzene and *n*-butyl acrylate.[a]

Precatalyst	Cycle (% yield[b])														
	1	2	3	4	5	6	7	8	9	10	11	12	13	14	15
4[a]	97	99	99	99	97	96	95	94	92	91	90	88	85	83	79
$Pd(CH_3CN)_2Cl_2$[c]	99	93	85	71	68	44									

[a] Reaction conditions: iodobenzene = 0.0401 mmol; *n*-butyl acrylate = 0.0488 mmol; NPr_3 = 0.0802 mmol; catalyst loading = 11.05 mg (8 mol% Pd(II)); solvent = d^8-toluene (0.1 mL); reaction temperature = 108 °C; reaction time for each cycle = 30 min.
[b] Determined by ^{1}H NMR spectroscopy analysis.
[c] Reaction conditions: iodobenzene = 0.375 mmol; *n*-butyl acrylate = 0.45 mmol; ^{n}NPr$_3$ = 0.75 mmol; and 8 mol% $Pd(CH_3CN)_2Cl_2$ in 0.1 mL toluene at 110 °C for 6 h.

The palladium in $(RS)_1Au(SL)_1(SLPdCl_2)_{0.57}$ (**4**) could be quantitatively recovered as a soluble black colloid **5** with an average core diameter of 14.1 ± 3.4 nm (Fig. 4 and Table 1). The large change in particle size of the recovered catalyst **4** was believed due to the Ostwald ripening phenomenon [55] observed at elevated temperature. These recovered particles were not only dissolvable but also precipitable, so they could be easily studied by solution-phase spectroscopy such as NMR and UV–vis; the solid form was studied by TEM, IR and XPS spectroscopy. The ^{1}H NMR spectra of **5** (Fig. 1e) clearly showed two different sets of supported pyridyls (i.e., of the uncapped Au–SL and the Pd^0-capped Au–SL–Pd^0) in a ratio of 1:0.53. Expectedly, the pyridyl protons of Au–SL–Pd^0 were shifted upfield to the Pd(II)-capped pyridyls of Au–SL–$PdCl_2$ in **4**. As elucidated earlier for **4**, the IR spectra of **5** (Fig. 2a) also gave a pyridyl ring stretching of ν_{py} at 1590 cm^{-1}, which indicated its covalent binding to palladium. The UV–vis spectra of **5** (Fig. 3) gave the characteristic Au surface-plasmon resonance peak at about 530 nm. The XPS spectroscopic analysis of a 1:1 mixture of **4** and **5** clearly gave two sets of BE for the Pd $3d_{3/2}$ and $3d_{5/2}$ levels, whereas the Pd^{II} BE levels of **4** were located at 343 and 337 eV, and the Pd^0 levels of **5** were located at 341 and 335 eV; these data are all consistent with previously reported values [38]. The BE of the gold $4f_{5/2}$ and $4f_{7/2}$ levels of the Au core in **5** were found at 88 and 84 eV, respectively. The combined spectral analyses of the recovered colloids **5** established that active palladium in the form of Pd^0 was bound to the Au NP surface dipyridyls. We therefore calculated the surface composition of **5** as $(RS)_xAu(SL)_1(SL–Pd^0)_{0.53}$ according to its XPS and ^{1}H NMR spectra, where the ratio ***x*** of octanethiolate (RS) was not determined as its NMR signal overlapped with the protons of the NPr_3·HI salt formed during catalysis. These results are theoretically consistent with the Pd(0)/Pd(II) catalytic cycle proposed for Heck reactions in the literature [56–59].

In addition, the recovered $(RS)_xAu(SL)_1(SL–Pd^0)_{0.53}$ was nonleaching and could be consecutively recycled in toluene with conversions maintained at >90% for the first 11 cycles, gradually dropping to 82% at the 15th cycle (Fig. 6 and Table 3). More importantly, the catalyst-recycling procedures for **5** were easy and sustainable, comprising only centrifugation and filtration. In contrast, the recycling of a molecular $Pd(CH_3CN)_2Cl_2$ catalyst requires multiple cycles of extraction with organic solvents followed by evaporation of organic volatiles. Under similar recycling conditions, the conversion for a system using $Pd(CH_3CN)_2Cl_2$ as the catalyst dropped from 99% to 85% on the 3rd cycle and to 44% on the 6th cycle. Fully palladated Au NP–Pd could also be reused many times; however, a gradual drop in conversion due to the small amount of Pd leaching during consecutive recycling procedures was noticed.

4. Conclusions

The main purpose of using Au NPs as a metal-complex catalyst support is to provide a good quality surface for the immobilization of metal complexes. By controlling the amount of palladium complex immobilized on the Au surface, the resulting hybrid catalyst can be imbued with a solubility generally obtained for the molecular system. As a result, the structural details and reaction chemistry of the hybrid catalyst systems can be easily studied and closely monitored. Consequently, more general conclusions and fundamental insights can be readily obtained. Leaving a certain portion of the surface-spacer-linkers uncapped allowed them to stably trap the active Pd(0) centers and to tightly bind leached Pd species during each catalytic cycle. This approach opens up a new avenue for the immobilization of metal-complex catalysts on the surface of MNPs in a well-defined manner. This method can also minimize the problem of metal leaching. In addition, adding Au NPs to the molecular Pd complex through a step-wise immobilization processes can promote further reactivity and can offer the advantages of quantitative recovery, effective recyclability and easy separation. We believe that the results of this study can serve as an important reference work for scientists active in organic synthesis, green catalysis, nanoscience and related areas, and it is expected that many applicable catalysts of this form can be made by tethering various metal complexes or even organocatalysts onto MNPs in a well-defined and controllable way so as to promote chemical reactions in a greener and more manageable fashion.

Acknowledgments

Funding for this work was provided by the National Science Council of Taiwan (NSC-97-2113-M-194-010-MY2), for which the authors are grateful. The authors are also grateful to the NSC South Precision Instrument Centers at National Chung Cheng University for performing the XPS experiments and at National Chung Hsing University for performing the ICP-MS spectral analysis.

References

[1] C.-B. Hwang, Y.-S. Fu, Y.-L. Lu, S.-W. Jang, P.-T. Chou, C.-R.C. Wang, S.J. Yu, J. Catal. 195 (2000) 336.
[2] D. Astruc, F. Lu, J. Ruiz Aranzaes, Angew. Chem. Int. Ed. 44 (2005) 7399.
[3] J.G. De Vries, Dalton Trans. (2006) 421.
[4] D. Astruc, Inorg. Chem. 46 (2007) 1884.
[5] G.A. Somorjai, A.M. Contreras, M. Montano, R.M. Rioux, Proc. Natl. Acad. Sci. USA 103 (2006) 10577.
[6] D. Astruc, F. Lu, J.R. Aranzaes, Angew. Chem. Int. Ed. 44 (2005) 7852.
[7] N. Toshima, Y. Shiraishi, T. Teranishi, M. Miyake, T. Tominaga, H. Watanabe, W. Brijoux, H. BJnnemann, G. Schmid, Appl. Organomet. Chem. 15 (2001) 178.
[8] G. Schmid, Chem. Rev. 192 (1992) 1709.
[9] R. Terril, T. Postlethwaite, C. Chen, C. Poon, A. Terzis, A. Chen, J. Hutchinson, M. Clark, G. Wignall, J. Londono, R. Superfine, M. Falvo, C.S. Johnson Jr., E. Samulski, R. Murray, J. Am. Chem. Soc. 117 (1995) 12537.
[10] M. Brust, D. Bethell, D.J. Schiffrin, C.J. Kiely, Adv. Mater. 7 (1995) 795.
[11] R.L. Whetten, J.T. Khoury, M.M. Alvarez, S. Murthy, I. Vezmar, Z.L. Wang, P.W. Stephens, C.L. Cleveland, W.D. Luedtke, U. Landmann, Adv. Mater. 8 (1996) 428.
[12] Y.-Y. Lin, S.-C. Tsai, S.J. Yu, J. Org. Chem. 73 (2008) 4920.
[13] Y. Uozumi, Y.M.A. Yamada, C.K. Jin, Synfacts 9 (2008) 995.
[14] T. Belser, M. Stöhr, A. Pfaltz, J. Am. Chem. Soc. 127 (2005) 8720.
[15] F. Ono, S. Kanemasa, J. Tanaka, Tetrahedron Lett. 46 (2005) 7623.
[16] M. Bartz, J. Küther, R. Seshadri, W. Tremel, Angew. Chem. 110 (1998) 2646.
[17] H. Li, Y.-Y. Luk, M. Mrksich, Langmuir 15 (1999) 4957.
[18] K. Marubayashi, S. Takizawa, T. Kawakusu, T. Arai, H. Sasai, Org. Lett. 5 (2003) 4409.
[19] R.F. Heck, J. Am. Chem. Soc. 90 (1968) 5518.

[20] A. Fihri, P. Meunier, J.-C. Hierso, Coord. Chem. Rev. 251 (2007) 2017.
[21] L. Yin, J. Liebscher, Chem. Rev. 107 (2007) 133.
[22] J.P. Knowles, A. Whiting, Org. Biomol. Chem. 5 (2007) 31.
[23] N.T.S. Phan, M. Van Der Sluys, C.W. Jones, Adv. Synth. Catal. 348 (2006) 609.
[24] W.A. Herrmann, C. Broβmer, K. Öfele, M. Beller, H. Fischer, J. Organomet. Chem. 491 (1995) C1.
[25] P. Nilsson, O.F. Wendt, J. Organomet. Chem. 690 (2005) 4197.
[26] F. d'Orlye, A. Jutand, Tetrahedron 61 (2005) 9670.
[27] K. Yu, W. Sommer, M. Weck, C.W. Jones, J. Catal. 226 (2004) 101.
[28] X.-S. Zhou, Z.-R. Dong, H.-M. Zhang, J.-W. Yan, J.-X. Gao, B.-W. Mao, Langmuir 23 (2007) 6819.
[29] Y.-F. Han, Z. Zhong, K. Ramesh, F. Chen, L. Chen, T. White, Q. Tay, S.N. Yaakub, Z. Wang, J. Phys. Chem. C 111 (2007) 8410.
[30] F.H.B. Lima, J. Zhang, M.H. Shao, K. Sasaki, M.B. Vukmirovic, E.A. Ticianelli, R.R. Adzic, J. Phys. Chem. C 111 (2007) 404.
[31] L. Djakovitch, K. Köhler, J. Am. Chem. Soc. 123 (2001) 5990.
[32] K. Köhler, R.G. Heidenreich, J.G.E. Krauter, M. Pietsch, Chem. Eur. J. 8 (2002) 622.
[33] S.S. Prockl, W. Kleist, M.A. Gruber, K. Köhler, Angew. Chem. Int. Ed. 43 (2004) 1881.
[34] S. Komiya, Synthesis of Organometallic Compounds: A Practical Guide, John Wiley and Sons, NY, USA, 1997. p. 249.
[35] D.V. Leff, C. Ohara, J.R. Heath, W.M. Gelbart, J. Phys. Chem. 99 (1995) 7036.
[36] Y.-S. Fu, S.J. Yu, Angew. Chem. Int. Ed. Engl. 40 (2001) 437.
[37] G. Beamson, D. Briggs, High Resolution XPS of Organic Polymers. The Scienta ESCA 300 Database, J. Wiley & Sons, Chichester, New York, Brisbane, Toronto, Singapore, 1992, ISBN 0-471-93592-1. p. 278.
[38] G. Kumar, J.R. Blackburn, R.G. Albrtdge, W.E. Moddeman, M.M. Jones, Inorg. Chem. 11 (1972) 296.
[39] M.S. Yoon, D. Ryu, J. Kim, K.H. Ahn, Organometallics 25 (2006) 2409.
[40] C.-G. Yang, C. He, J. Am. Chem. Soc. 127 (2005) 6966.
[41] R. Abel, P. Collins, K. Eichler, I. Nicolau, D. Peters, in: G. Ertl, H. Knözinger, J. Weitkamp (Eds.), Handbook of Heterogeneous Catalysis, vol. 5, Wiley VCH, Germany, 1997, p. 2298.
[42] A.M. Venezia, V. La Parola, V. Nicoli, G. Deganello, J. Catal. 212 (2002) 56.
[43] D.L. Trimm, Z.I. Onsan, Catal. Rev. 43 (2001) 31.
[44] M. Chen, D. Kumar, C.-W. Yi, D.W. Goodman, Science 310 (2005) 291.
[45] M. Bartz, J. Küther, R. Seshadri, W. Tremel, Angew. Chem. Int. Ed. 37 (1998) 2466.
[46] M. Beller, H. Fisher, K. Kuhlein, C.-P. Reisinger, W.A. Herrmann, J. Organomet. Chem. 520 (1996) 257.
[47] J. Tsuji, Palladium Reagents and Catalysts, Wiley, New York, 1995. p.125 (Chapter 4).
[48] I.P. Beletskaya, A.V. Cheprakov, Chem. Rev. 100 (2000) 3009.
[49] M. Albrecht, G. van Koten, Angew. Chem. Int. Ed. 40 (2001) 3750.
[50] B.M. Choudary, S. Madhi, N.S. Chowdari, M.L. Kantam, B. Sreedhar, J. Am. Chem. Soc. 124 (2002) 14127.
[51] P. Mehnert, D.W. Weaver, J.Y. Ying, J. Am. Chem. Soc. 120 (1998) 12289.
[52] A.F. Shmidt, L.V. Mametova, Kinet. Catal. 37 (1996) 406.
[53] F. Zhao, B.M. Bhanage, M. Shirai, M. Arai, Chem. Eur. J. 6 (2000) 843.
[54] A. Biffis, A.M. Zecca, M. Basato, Eur. J. Inorg. Chem. (2001) 1131.
[55] L. Ratke, P.W. Voorhees, Growth and Coarsening: Ostwald Ripening in Material Processing, Springer, 2002, ISBN 3-540-42563-2. pp. 117–118.
[56] G.T. Crisp, Chem. Soc. Rev. 27 (1998) 427.
[57] C. Amatore, A. Jutand, Acc. Chem. Res. 33 (2000) 314.
[58] M. Buback, T. Perkovic, S. Redlich, A. de Meijere, Eur. J. Org. Chem. (2003) 2375.
[59] C.S. Consorti, F.R. Flores, J. Dupont, J. Am. Chem. Soc. 127 (2005) 12054.